Organic & Biomolecular Chemistry

This article is part of the

OBC 10th anniversary

themed issue

All articles in this issue will be gathered together online at

www.rsc.org/OBC10

Organic & Biomolecular Chemistry

Dynamic Article Links
View Online

Cite this: *Org. Biomol. Chem.*, 2012, **10**, 6159

www.rsc.org/obc

PAPER

Multimodal fluorescence modulation using molecular photoswitches and upconverting nanoparticles†‡

Carl-Johan Carling, John-Christopher Boyer and Neil R. Branda*

Received 21st February 2012, Accepted 22nd March 2012
DOI: 10.1039/c2ob25368b

The intensity and colour of the light emitted from upconverting nanoparticles is controlled by the state of photoresponsive dithienylethene ligands decorated onto the surface of the nanoparticles. By selectively activating one or both ligands in a mixed, 3-component system, a multimodal read-out of the emitted light is achieved.

Introduction

Nanoscale fluorescent probes decorated with photoresponsive organic ligands offer heightened control in optical materials applications by reversibly turning the emission signal 'on' or 'off', or by modulating the visual output from one colour to another.[1–14] Both optical properties are based on the photoresponsive ligands undergoing controlled and predictable reactions between two isomers having different optoelectronic characteristics.[15] Hybrid systems that have these properties have the potential to advance technologies such as non-destructive ultra-dense optical memory[8,10] and bio-imaging.[3,4,12–14] The latter application is a particularly appealing use for these optical probes as it offers advantages over conventional systems when false-positive signals need to be better identified. Temporal tracking of the nanoparticles is also possible when the end-user can control the optical signal 'on command'.[16]

Both organic and organic–inorganic hybrid nanoparticles have been developed for modulating fluorescence but limitations in the current technology still exist. One of the major limitations is the need for high-energy light as the fluorescence excitation source, which causes auto-fluorescence of bio-molecules and non-selective photoswitching of the organic ligands since the ligands absorb in the same spectral regions as the source. Non-selective photoswitching could potentially lead to distortions of the fluorescent signal during prolonged excitation due to unwanted organic photoreactions and subsequent degradation of the signal quality. Because many photoresponsive systems such as spiropyrans and spirooxazines were designed to undergo spontaneous reactions (T-type photochromic compounds), their use in temporal imaging studies is less appealing than compounds that exhibit bistability over a wide range of temperatures. The last limitation relevant to discuss in the context of this manuscript is the fact that fluorescent probes based on organic compounds are prone to photo-degradation, which limits the time they can be used in imaging applications. Although quantum dots have been demonstrated as a viable solution to this problem, their blinking behavior and toxicity (unless specially coated) limits their use as well.[17]

These limitations can be avoided by developing hybrid systems based on lanthanide-doped upconverting nanoparticles (UCNP) decorated with 'thermally stable' P-type dithienylethene photochromic ligands, which can modulate the multi-photon NIR-to-visible emission. The nanoparticles can convert 980 nm light into several other types of light that are emitted in the UV, visible and NIR regions of the spectrum.[18] They are also non-toxic and do no exhibit blinking.[19–21] Photoresponsive dithienylethene derivatives are one of the most versatile class of photochromic compounds.[22] They undergo predictable ring-closing and ring-opening reactions when stimulated with UV and visible light, respectively, often with a high degree of fatigue resistance (see the bottom of Scheme 1 for an example of this reaction). The combination of these inorganic and organic systems is well suited to address the limitations described above.

We recently reported an example of 'on command' fluorescence modulation *in vivo* using a dithienylethene–UCNP hybrid system.[14] In this manuscript, we describe our more advanced systems where a heightened level of control over the emission intensity and wavelength, and colour output is achieved by decorating the nanoparticles with pure or mixed dithienylethene ligands. We chose to use one of our recently developed *core–shell–shell* upconverting, multi-colour nanoparticles[23] in combination with two different dithienylethene chromophores to photo-modulate the NIR-to-visible fluorescence of the UCNP (**1a-NP**, **1b-NP** and **1ab-NP**, Scheme 1). By taking advantage of the multi-colour nature of the upconverted fluorescence and the fact that the two dithienylethenes can be

4D LABS, Department of Chemistry, Simon Fraser University, 8888 University Drive, Burnaby, B.C., Canada. E-mail: nbranda@sfu.ca; Fax: +1 778 7823765; Tel: +1 778 7828061

† This article is part of the *Organic & Biomolecular Chemistry* 10th Anniversary issue.

‡ Electronic supplementary information (ESI) available: Spectroscopy of new and key compounds and photochemical studies. See DOI: 10.1039/c2ob25368b

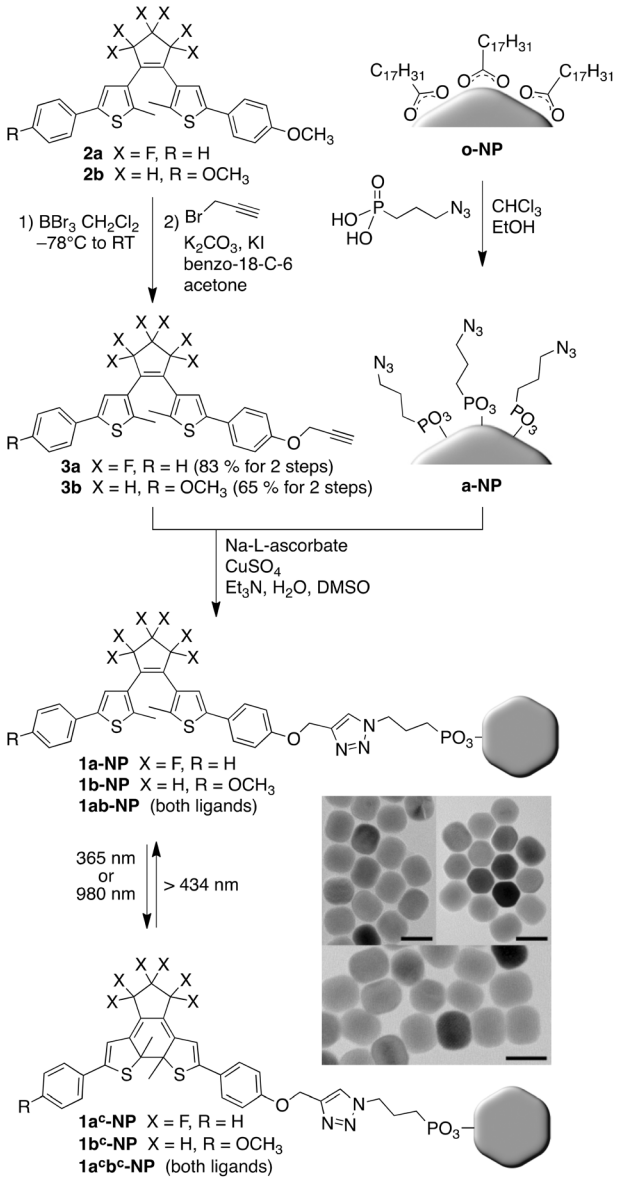

Scheme 1 Synthesis of photoresponsive ligands **3a** and **3b**, the azide-functionalized *core–shell–shell* UCNPs **a-NP**, and the hybrid one- and two-component systems **1a-NP**, **1b-NP** and **1ab-NP**. The reversible photoreactions of the three systems using UV, visible and NIR light are also shown. The insets show the TEM images of the nanoparticles in their different decorated forms (**1a-NP**, top left; **1b-NP**, top right; **1ab-NP**, bottom). The scale bars in all 3 images represent 40 nm.

selectively activated using specific wavelengths of light, we demonstrate selective quenching of the emission and multimodal modulation. We also show that we can trigger the ring-closing of the photoswitches in a 'remote-control' manner by increasing the power density of the NIR excitation source and using the multi-photon NIR-to-UV emission from the nanoparticles.

Results and discussion

Synthesis of dithienylethene ligands and decorated nanoparticles

The hybrid 2- and 3-component chromophore–UCNP systems were prepared as shown in Scheme 1. The photoresponsive ligands, **3a**[24] and **3b**, bearing the alkyne group necessary for the copper(I)-catalyzed azide–alkyne cycloaddition (CuAAC) 'click' reaction were synthesized in two steps from the known dithienylethenes **2a**[25] and **2b**[26] and characterized by ^{1}H and ^{13}C NMR spectroscopy, mass spectrometry and UV-vis absorption spectroscopy. The azide coated *core–shell–shell* upconverting nanoparticles, **a-NP** were prepared through a ligand-exchange reaction[14] by stirring the previously reported oleate coated **o-NP**[23] with azidopropylphosphonate[27] in $CHCl_3$ and ethanol. The composition of these UCNPs is β-$NaYF_4$: 0.5% Tm^{3+} : 30% Yb^{3+} in the *core*, β-$NaYF_4$: 2.0% Er^{3+} : 20% Yb^{3+} in the inner *shell* and β-$NaYF_4$ in the outer *shell*. These azide-decorated nanoparticles were characterized by IR spectroscopy, which showed a band in the spectrum at 2110 cm^{-1} corresponding to the azide N=N=N stretch (Fig. S1‡).[28] The photoresponsive organic chromophores were attached to the surface of the nanoparticles using CuAAC 'click' chemistry.[29] Treating **a-NP** with pure **3a**, pure **3b** or a mixture of both acetylenes with a copper catalyst and an ascorbate reductant afforded the two 2-component systems **1a-NP** and **1b-NP**, and the 3-component system **1ab-NP**, respectively. All three hybrid systems were characterized by IR spectroscopy, transmission electron microscopy (TEM) (inset to Scheme 1), and UV-vis absorption and fluorescence spectroscopy. The success of the 'click' reaction was verified by the almost complete disappearance of the azide N=N=N stretch at 2110 cm^{-1} in the IR spectrum (Fig. S1‡).

Absorption spectroscopy and selective quenching of emission

Inconveniently, the two 2-component hybrid systems, **1a-NP** and **1b-NP**, could not be dispersed in the same solvent for characterization. Although the ligands (**3a** and **3b**) were freely soluble in CH_3CN, the solvent in which most of the photochromic studies were carried out (Fig. S2‡),[28] neither **1a-NP** nor **1b-NP** could be dispersed in CH_3CN. Other organic solvents worked well, and **1a-NP** and **1b-NP** formed clear colloidal suspensions in THF and in CH_2Cl_2, respectively. The mixed 3-component system (**1ab-NP**) formed a faintly hazy colloidal dispersion in THF. These solvents were used for all studies described in this paper.[30]

The UV-vis absorption spectra of the 2-component systems (**1a-NP** and **1b-NP**) are shown in Fig. 1 along with the emission spectra of the UCNPs in the various states based on the photoresponsive ligands and the power of the 980 nm excitation light. These spectra illustrate our design principle and our rationale for choosing the specific nanoparticles and photoresponsive ligands. When the dithienylethenes are in their ring-open forms (**1a-NP** and **1b-NP**), they absorb only in the UV region of the spectrum (<400 nm). These absorption bands decrease when the solutions are irradiated with UV light (365 nm) as is typical for dithienylethene derivatives (Fig. 1a and 1b, and Fig. S4‡).[28] This decrease is accompanied by the appearance of broad bands in the visible region of the spectrum as the ring-open isomers are converted into their ring-closed counterparts (**1a-NP** → **1a^{c}-NP** and **1b-NP** → **1b^{c}-NP**). These changes account for the change in colour of the solutions from colourless to blue in the case of **1a-NP** and red in the case of **1b-NP**. Although the amount of ring-closed isomers in the photostationary states cannot be

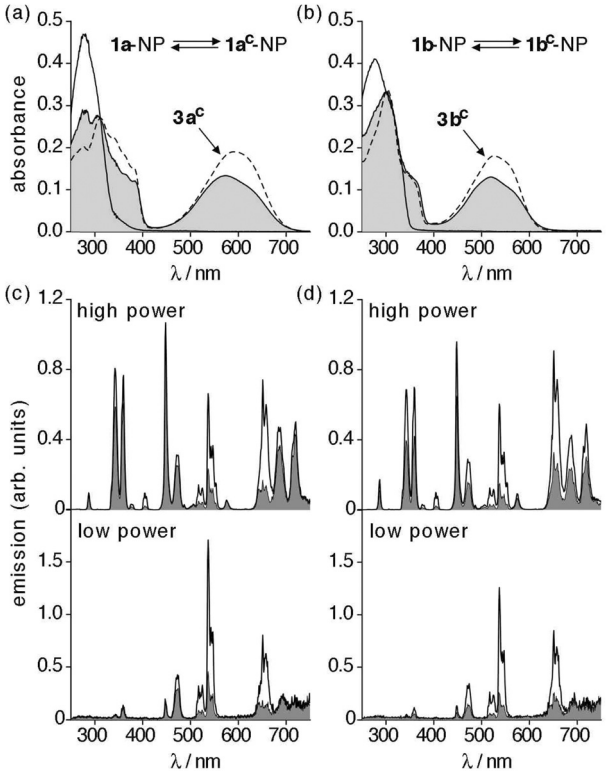

Fig. 1 UV-vis absorption spectra of solutions (10^{-5} M) of one-component systems (a) **1a-NP** (THF) and (b) **1b-NP** (CH_2Cl_2) before (solid lines) and after irradiation with 365 nm (16 mW cm^{-2}) light (shaded areas) for 120 s. The spectra for the ligands (**3a** and **3b**) are shown for comparison (dashed lines). The molar concentration refers to the estimated amount of photoswitch in each sample,[32] while the amount of decorated nanoparticle in each solution is 0.05 wt% for **1a-NP** and 0.03 wt% for **1b-NP**. Emission spectra of the same solutions (λ_{ex} = 980 nm) of (c) **1a-NP** and (d) **1b-NP** at high 980 nm excitation power (38 W cm^{-2}, top graphs) and low 980 nm excitation power (2 W cm^{-2}, bottom graphs) showing how the intensity of specific bands in the original emission spectrum (white areas) are reduced when the photoswitches are converted into their ring-closed forms (shaded areas) based on the overlap with the absorption bands of **1a^c-NP** and **1b^c-NP**.

conveniently measured on the decorated nanoparticles, we can only make the assumption that they are similar to those for similar solutions of the ligands, which were measured by ^{1}H NMR spectroscopy to be 72% and 56% for **3a^c** and **3b^c**, respectively. When the coloured solutions of **3a^c** and **3b^c** are irradiated with visible light at wavelengths greater than 434 nm, the colours of the solutions return to their original states and the ring-open isomers are regenerated.[31]

A closer inspection reveals that the absorption spectra for the ring-closed isomers decorated on the nanoparticles are not identical to those for the free ligands (Fig. 1a and b, and Fig. S2 and S4‡). In both cases, the absorption bands appear to have more pronounced features. Peak fitting the bands (Fig. S5‡) shows that none of them are Gaussian in shape. Instead, they are comprised of at least 3 overlapping bands corresponding to an equivalent number of electronic transitions. The difference between the electronic properties of the ring-closed isomers when free or anchored to the nanoparticles must be due to the non-equivalent shifting of each of these overlapping bands a phenomenon we also noticed was present in our previously reported system.[14] The exact reason for these spectral changes is not clear at this stage, although it likely results from the electronic coupling between the nanoparticle and the ring-closed chromophores in their ground states.

The number of molecules of each photoresponsive ligand was calculated by estimating the concentration of organic ligands based on their UV-vis spectra and measuring the dimensions of the nanoparticles using their TEM images. This calculation resulted in an estimated loading of approximately 5000–7000 molecules per nanoparticle for both **1a-NP** and **1b-NP**.[28] In the case of the mixed, 3-component system (**1ab-NP**), which will be discussed later in this paper, the ratio of the chromophores **1a** and **1b** was calculated to be approximately 5 : 4 (Fig. S6‡),[28] which corresponds to an approximate loading of approximately 10 000 molecules of **1a** and **1b** per nanoparticle.

We chose these two photoresponsive compounds because they have similar absorption spectra in their ring-open forms but differ significantly in their ring-closed counterparts. These features make them ideal for decorating them onto multi-wavelength emitting UCNPs to offer a heightened level of control over the emissive properties of the nanoparticles compared to our previous version.[14] Our *core–shell–shell* UCNPs[23] have six major emissions in the UV-vis regions of the spectrum when excited at high 980 nm power density as shown in Fig. 1c and 1d. These emissions are due the different states of the lanthanide dopants: Tm^{3+} (UV, blue, red and NIR) and Er^{3+} (green and red) as previously reported.[23] The longer wavelength emission bands (670–750 nm) visible in the wavelength-sensitivity corrected spectra upon high power density 980 nm excitation are not true emissions but are the second order diffraction of the UV Tm^{3+} emissions off the grating of the emission monochromator and should be ignored.[33] We[23] and others[34,35] have mistakenly acknowledged these red emissions as real.

Fig. 1c–d illustrate our ability to modulate the emissions from the UCNPs depending on the state of the photoresponsive ligands and the power density of the excitation light. When the ligands are in their colourless, ring-open states in **1a-NP** and **1b-NP**, the multi-photon emission from the nanoparticles is 'bright' when excited with high power 980 nm light (38 W cm^{-2}) and slightly less bright when the power is lowered (2 W cm^{-2}). Because there are three major visible emissions present (blue, green and red) under high excitation power, the fluorescence is perceived as white light. When the power is lowered, the colour appears green. When the photostationary states are produced by exposing the systems to 365 nm light, the emissions from **1a^c-NP** and **1b^c-NP** are quenched under both high and low 980 nm excitation power (Fig. 1c and d). We ascribe this fluorescence quenching effect to a combination of resonance energy transfer and an inner filter effect from nearby nanoparticles.

Although both ligands quench the nanoparticle's emission in their ring-closed forms, they do so to different degrees and are wavelength dependent (Fig. 1 and Table 1). Both **3a^c** and **3b^c** have absorbance bands in the 350–400 nm region of the spectrum, which overlap with the UV emissions from the nanoparticles. Therefore, they both reduce the intensity of these emissions. In the case of compound **3a^c**, which is blue in colour due to its absorbing between 430–720 nm with absorption

Table 1 The differences in the intensities for the specific bands for each lanthanide ion transition in the emission spectra of the solutions of **1a-NP** and **1b-NP** used in Fig. 1 and 2 when the chromophores are converted into their ring-closed forms using 365 nm light

				% Of original emission[a]			
				High-intensity NIR light[b]		Low-intensity NIR light[b]	
Emitting ion	Transition	Number of photons	λ_{em} (nm) (λ_{ex} = 980 nm)	**1a^c-NP**	**1b^c-NP**	**1a^c-NP**	**1b^c-NP**
Tm^{3+}	$^3P_0 \rightarrow {}^3H_6$	5	276–292	0	69	—	—
Tm^{3+}	$^3P_0 \rightarrow {}^3F_4$	5	323–351	73	57	96	82
Tm^{3+}	$^1D_2 \rightarrow {}^3H_6$	4	352–368	80	60	80	59
Er^{3+}	$^2H_{9/2} \rightarrow {}^4I_{15/2}$	4	392–411	26	26	—	—
Tm^{3+}	$^1D_2 \rightarrow {}^3F_4$	4	430–457	93	66	85	67
Tm^{3+}	$^1G_4 \rightarrow {}^3H_6$	3	458–486	82	54	71	47
Er^{3+}	$^2H_{11/2}$, $^4S_{3/2} \rightarrow {}^4I_{15/2}$	2	501–562	37	27	29	26
Er^{3+}	$^4F_{9/2} \rightarrow {}^4I_{15/2}$	2	626–670	30	39	35	39
Tm^{3+}	$^1G_4 \rightarrow {}^3I_4$	3					
	Total		276–670	53	50	66	53

[a] Values are based on the areas under the curves for each spectral region. The bands from 671–750 nm were not included in the analysis because these emissions are due to the second order diffraction of the upconverted UV light off the grating of the emission monochromator. [b] High-intensity light = 38 W cm^{-2}. Low-intensity light = 2 W cm^{-2}. The nomenclature, **1a^c-NP** and **1b^c-NP** refer to the photostationary states containing an estimated 72% and 56% of the ring-closed isomers, respectively.

maxima centered at 592 nm, the green and red emissions are also reduced. When this occurs, the colour of the emitted light from **1a^c-NP** appears blue as shown in Fig. S7 and S8.‡[28] The ring-closed chromophore in **1b^c-NP** also quenches the green emission. However, because absorption bands of **1b^c-NP** are blue shifted (420–640 nm with absorption maxima centered at 521 nm) with respect to those of **1a^c-NP**, the extent of quenching is not the same. In this case, there is less quenching of the longer wavelength emissions and more or the shorter wavelength ones. Although the absorption bands of **1b^c-NP** do not overlap with the red emission, it is still quenched in **1b^c-NP** due to the fact that the excited state responsible for the green emission ($^2H_{11/2}$, $^4S_{3/2}$) in Er^{3+} is partially populating the lower energy state ($^4F_{9/2}$) from which the red light is emitted through a nonradiative decay process. Due to the low absorption for both chromophores in the 400–450 nm region of the spectrum, neither effectively quenches the blue emissions to a large extent.

An interesting observation is the quenching of the highest energy UV emission bands, which is less in **1a^c-NP** than in **1b^c-NP** even though the relative overlap of the two systems are similar. We suspect that the quenching of the blue emissive states also quenches the UV states by preventing excited Tm^{3+} ions from reaching higher excited states.

When the power density of the 980 nm excitation source is reduced from 38 W cm^{-2} to 2 W cm^{-2}, the UV and visible emissions from the *core–shell–shell* UCNP change as we have previously demonstrated.[23] The underlying reason for this behavior is the fact that the very strong two-photon upconverted 800 nm emission from Tm^{3+} dominates at lower power densities and the UV and visible emissions from Tm^{3+} almost cease. As a result, at low 980 nm power density, the primary visible light emitter is Er^{3+}. Fig. 1c and 1d show how these emissions are similarly modulated by the state of the photoswitches decorated on to their surfaces. The quenching behavior of the ring-closed forms **1a^c-NP** and **1b^c-NP** at low power density excitation is similar to those observed at high power density. It is primarily the emission from Er^{3+} that is quenched by the photoswitches (Fig. 1 and Table 1).

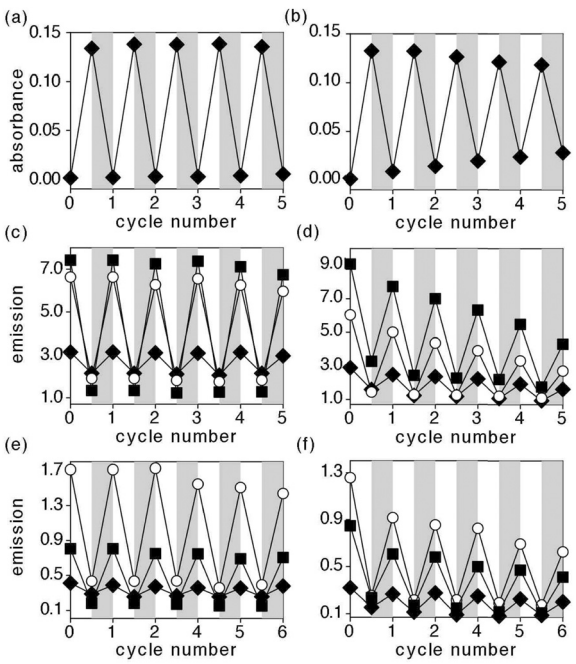

Fig. 2 Changes in the absorbances at (a) 570 nm when the same solution of **1a-NP** used in Fig. 1(a,c) and (b) 520 nm when the same solution of **1b-NP** used in Fig. 1(b,d) are irradiated alternately with 365 nm light (16 mW cm^{-2}) for 120 s for **1a-NP** and 130 s for **1b-NP** (white areas), and >434 nm (377 mW cm^{-2}) light for 60 s for **1a-NP** and 120 s for **1b-NP** (shaded areas). (c–f) Changes in the emission intensities at 471 nm (♦), 537 nm (■) and 651 nm (◯) when the same solutions are irradiated under identical conditions at (c,d) high 980 nm excitation power and (e,f) low 980 nm excitation power.[36]

As is the case for the ring-closed forms of the ligands (**3a^c** and **3b^c**), irradiating solutions of the equivalent ring-closed

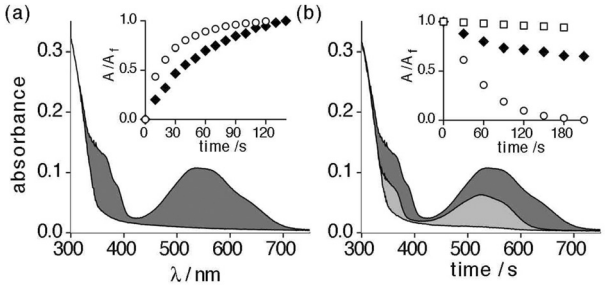

Fig. 3 (a) The UV-vis absorption spectrum of a THF solution of the two-component hybrid system **1ab-NP** before (white) and after (dark shaded) irradiation with 365 nm light (16 mW cm^{-2}). The total concentration of chromophore is 10^{-5} M (in a 5 : 4 **1a** : **1b** ratio), while the amount of decorated nanoparticle is 0.03 wt%. The inset shows the time-dependent growth of the absorptions at 570 nm (◯) and 520 nm (♦) corresponding to the two ring-closed isomers in **1a^{c}b^c-NP**. (b) The UV-vis absorption spectrum of the same photostationary state before (dark shaded), after irradiation with >630 nm light (120 mW cm^{-2}) (light shaded) and after irradiation with >434 nm light (377 mW cm^{-2}) (white). The inset shows the time-dependent changes of the absorptions at 570 nm (◯) and 520 nm (♦) during the >630 nm irradiation, and at 520 nm (□) for a CH_3CN solution of ligand **3b** (1.0×10^{-5} M) when it is irradiated with >630 nm light.

systems **1a^c-NP** and **1b^c-NP** with visible light of wavelengths greater than 434 nm triggers the reverse photoreaction and quantitatively regenerates the ring-open isomers. It also restores the original bright emissive states of the nanoparticles. Both systems could be cycled between a bright and quenched emissive states several times by alternating the type of light (Fig. 2c–f), although significant degradation of the signal was observed in the case of **1b-NP**. The absorption corresponding to this less robust photoswitch is also reduced upon cycling (Fig. 2a and b) showing that the reduced performance is due to degradation of the ligand.

Selective photochromism and quenching in the mixed system

The fact that the two ring-closed isomers absorb in different regions of the visible spectrum implies that they can be selectively activated. This concept is demonstrated using the mixed, 3-component system **1ab-NP**. Fig. 3 shows how the photoresponsive chromophores can be independently addressed.[37] As expected, the absorption spectra of both the ring-open and ring-closed states of the mixed system are equivalent to the sum of the two systems. When both ring-open isomers are present (**1ab-NP**), there are no bands in the visible region of the spectrum. Exposure to UV light (365 nm) activates both chromophores, generates the mixed photostationary state and produces broad absorbances in the visible region (Fig. 3a). Although there appears to be a slight difference in the growth of the absorbances corresponding to each isomer (570 nm for the equivalent of **1a-NP** and 520 nm for the equivalent of **1b-NP**) as shown in the inset to Fig. 3a, this may be due to slight differences in the amount of light absorbed by each chromophore.

Because the ring-closed form of the chromophore in **1a^c-NP** absorbs longer wavelength of light to trigger the ring-opening reaction than the chromophore in **1b^c-NP**, it can be selectively activated using light at wavelengths greater than 630 nm as shown in Fig. 3b. Irradiation at these wavelengths results in the decrease in the longer wavelength absorptions while retaining the shorter wavelength ones. This state corresponds to one where only the blue-shifted chromophore is in its ring-closed state (**1ab^c-NP**). The inset to Fig. 3b shows that the wavelengths corresponding to each isomer are reduced in intensity to a different extent during the >630 nm exposure. While that corresponding to the red-shifted chromophore (570 nm) is completely reduced, those corresponding to the blue-shifted isomer and the corresponding ligand (**3b^c**) are insignificantly reduced. Irradiation of this state with light at wavelengths longer than 434 nm activates the blue-shifted chromophore and regenerates the original system.

The four different states of the mixed, 3-component system are illustrated in Scheme 2. While the all ring-closed state (**1a^{c}b^c-NP**) and the state where the red-shifted chromophore is ring-opened (**1ab^c-NP**) can be accessed, the latter can only be formed through the former owing to the fact that both dithienylethenes absorb in the same region of the UV spectrum in their ring-open forms, and therefore, cannot be independently activated. The state where the blue-shifted chromophore is ring-open and the red-shifted is ring-closed (**1a^{c}b-NP**) is not accessible because the ring-closed isomer of the red-shifted form also absorbs in the region between 450 and 500 nm.

By selectively activating the photoresponsive ligands in the mixed, 3-component system, their emission can also be regulated in a multi-modal fashion (Fig. 4, S13 and S14,‡ and Table 2). When both of the photoswitches are in their ring-open forms (**1ab-NP**), the observed multi-photon fluorescence is bright as is expected given the sum of the UV-Vis absorption spectra does not have bands in the visible region of the spectrum. When the photostationary state containing the ring-closed forms of both ligands (**1a^{c}b^c-NP**) is generated using 365 nm light, the broad absorption bands in the visible region of the spectrum result in the quenching of the emission from the UCNPs. The effect is synergistic since the sum of the absorption spectra of the two ligands absorbs across a wider region of the spectrum. There are two fates for this doubly ring-closed isomer depending on the light used to activate ring-opening as discussed above. Each has a different effect on the emission from the nanoparticles. As can be seen from Fig. 4c, S13 and S14,‡ and Table 2, not all emissions are equally sensitive to selective modulation and those arising from Er^{3+} appear to be the most effected.

'Remote-control' ring-closing

We have previously demonstrated that the light emitted from the UCNPs when excited with 980 nm light can be used to trigger the photochemical reactions of dithienylethenes[23,38] and 'caged' compounds.[39,40] They have subsequently been used by others for photoswitching[34] and photorelease.[35] This 'remote control' NIR-to-UV ring-closing is possible for the cases reported here although the power density of the 980 nm excitation source must be significantly increased in dilute conditions (Fig. 5 and S15‡). When solutions of either nanoparticle (**1a-NP** or **1b-NP**) is exposed to 980 nm light for prolonged periods of time, the solutions gradually changed to the coloured forms corresponding to

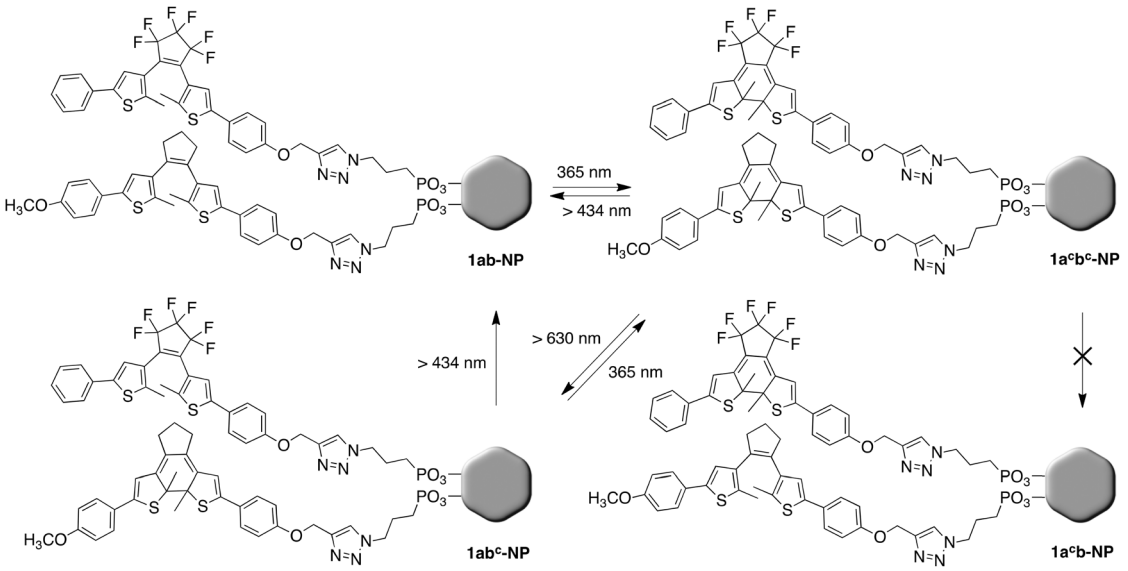

Scheme 2 Using 365 nm light, the three-component hybrid system (**1ab-NP**) can be converted into its coloured (violet) state where both photoswitches are in their ring-closed forms (**1a^{c}b^c-NP**). Long-wavelength visible light (>630 nm) selectively ring-opens the blue chromophore and generates the mixed system **1ab^c-NP**. Both photoswitches in **1a^{c}b^c-NP** or **1ab^c-NP** can be ring-opened back to **1ab-NP** using shorter-wavelength visible light (>434 nm). The **1a^{c}b-NP** cannot be accessed.

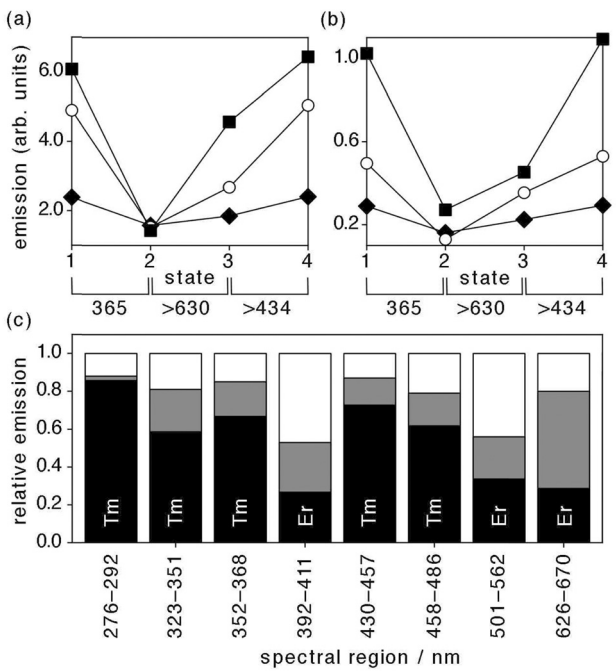

Fig. 4 Changes in the emission intensities at 471 nm (♦), 537 nm (■) and 651 nm (◯) when the same solution of **1ab-NP** used in Fig. 3 is exposed to 365 nm, >630 nm and >434 nm light at (a) high 980 nm excitation power and (b) low 980 nm excitation power. (c) Relative areas under the peaks in the emission spectra of the same solution before, (white) and after irradiation with 365 nm light (black) and >630 nm light (grey). High 980 nm excitation power was used in (c). In each case, the emitting ion is labelled.

Table 2 The differences in the intensities for the bands for each region in the emission spectra of the solution of **1ab-NP** used in Fig. 3 and 4 when the chromophores are converted into their specific ring-closed forms using 365 nm and > 630 nm light

	Relative emission[a]		
λ_{em} (nm)(λ_{ex} = 980 nm)	**1ab-NP**	**1a^{c}b^c-NP**[b]	**1ab^c-NP**[b]
276–292	1	0.86	0.88
323–351	1	0.59	0.81
352–368	1	0.67	0.85
392–411	1	0.27	0.53
430–457	1	0.73	0.87
458–486	1	0.62	0.79
501–562	1	0.34	0.56
626–670	1	0.29	0.80

[a] Values are based on the areas under the curves for each spectral region. High-intensity light (38 W cm^{-2}) excitation light was used. [b] These states refer to the photostationary states when the systems are irradiated with UV and visible light. They do not imply pure ring-closed isomers. The nomenclature, **1a^c-NP** and **1b^c-NP** refer to the photostationary states containing an estimated 72% and 56% of the ring-closed isomers, respectively.

the ring-closed states (blue for **1a^c-NP** and red for **1b^c-NP**). Due to presence of both UV and visible light in the multiphoton emissions, the photostationary states generated using 980 nm light will contain a lower amount of ring-closed isomers than the photostationary states generated using 365 nm light where no interfering visible emission is present.

Conclusions

We have shown here that depending on the choice of photoresponsive ligand anchored onto the surface of upconverting nanoparticles, multimodal regulation of the emission signal can be achieved. The 2-component systems (**1a-NP** and **1b-NP**) can

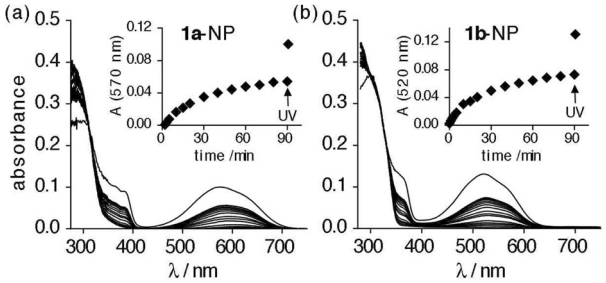

Fig. 5 Changes in the UV-vis absorption spectra when (a) a THF solution of **1a-NP** (10^{-5} M, 0.05 wt%) and (b) a CH_2Cl_2 solution of **1b-NP** (10^{-5} M, 0.03 wt%) are irradiated with 980 nm light (143 W cm^{-2}). The insets show the growth of the absorbances at 570 nm for **1a-NP** → **1a^c-NP** and 520 nm for **1b-NP** → **1b^c-NP** corresponding to the ring-closed isomers. The arrows in each inset plot indicate when the excitation light was changed from 980 nm to 365 nm.

be selectively toggled between a colourless, bright NIR-to-visible fluorescent state and a coloured, quenched state using light of different wavelengths than the fluorescence excitation light source. The modulated quenching of the two 2-component hybrid systems **1a^c-NP** and **1b^c-NP** was similar as they both primarily quench the green and red emissions of Er^{3+} over the blue emission of Tm^{3+}. Multimodal regulation of the 3-component hybrid system (**1ab-NP**) offers the ability to selectively alternate between three different fluorescent states due to the selective control over the **1a^c** → **1a** ring-opening reaction of **1a^{c}b^c-NP** using visible light of wavelengths greater than 630 nm. Although multiple fluorescent states were achievable using our photoswitches, they both primarily quench the emission from Er^{3+}. More distinct blue/white to green/white fluorescence modulation is achievable by selectively quenching the blue emissions of Tm^{3+} instead of the green and red emissions of Er^{3+} with a yellow-coloured ring-closed photoswitch.[41] These fluorescent hybrid systems have the capacity to be useful in various applications such as bio-imaging, non-destructive data storage and security.

Experimental

General methods

All reagents and solvents used for synthesis, chromatography, photochemistry and UV-vis spectroscopy measurements were purchased from Aldrich and used as received, unless otherwise noted. Anhydrous ethanol (EtOH) was purchased from Commercial Alcohols. Triethylamine was purchased from Anachemia. Anhydrous CH_2Cl_2 was purchased from Aldrich and passed through activated alumina using a solvent purification system before use. CD_2Cl_2 was purchased from Cambridge Isotope Laboratories and used as received. Column chromatography was performed using silica gel 60 (230–400 mesh) from Silicycle Inc. The oleate coated UCNPs (**o-NP**),[23] 3-azidopropylphosphonic acid,[27] and photoresponsive dithienethylethenes **2a**,[25] **2b**[26] and **3a**[24] were synthesized according to published procedures with slight modifications.

^{1}H NMR and ^{13}C NMR characterizations were carried out using a Bruker AVANCE III (5 mm TXI inverse probe) working at 500.19 MHz for ^{1}H- and at 125.77 MHz for ^{13}C NMR. Chemical shifts (δ) are reported in parts per million relative to tetramethylsilane using the residual solvent peak as a reference standard. Coupling constants (J) are reported in hertz. Melting points were measured using a Gallenkamp melting point apparatus (Registered Design No. 889339) and reported without correction. Exact mass measurements were done using a Kratos Concept-H instrument with perfluorokerosene as the standard. Photographs were taken with an Olympus E-410 digital single lens reflex camera fixed on a tripod and recorded with shutter speed: 1/80 and aperture: F5.6 for photos with ambient light on, and shutter speed: 1/2 and aperture: F5.6 for photos with the ambient light off. Laser and light power was measured on a Gentec TPM-300. The power density of the laser beam was calculated by dividing the recorded power by the laser beam area (focused beam (high power): filled circle, d: 0.6 mm, A: 0.028 cm^2, defocused beam (low power): hollow ellipse, a: 0.65 mm, b: 3 mm, A: 0.612 cm^2).

Transmission electron microscopy (TEM) and high-resolution TEM (HR-TEM) images were obtained using a Tecnai 200 keV Field Emission Scanning Transmission Electron Microscope. Dilute colloids of the NPs (0.1 wt%) dispersed in THF (**1a-NP**, **1ab-NP**) or toluene (**1b-NP**) were drop-casted on thin, carbon formvar-coated copper grids for imaging. The NP shape and crystallinity were evaluated from the collected TEM images, while the particle size was calculated from over 150 particles.

Spectroscopic studies

IR spectra were acquired on a Bomem (Hartmann & Braun, MB-Series) spectrometer. IR samples were prepared by mixing 1 part of dried, functionalized nanoparticles with 10 parts of KBr after which they were pressed into translucent discs. A Varian Cary 300 Bio spectrophotometer was used to acquire all UV-vis spectra. The nanoparticle samples were prepared by mixing 0.05 mL stock solution of **1a-NP**, **1b-NP** or **1ab-NP** with 3 mL of solvent in a square quartz fluorescence cuvette (1 × 1 × 4.5 cm). All volumes were measured out using 1 mL disposable syringes and 22 gauge needles. Emission spectra for solutions of **1a-NP**, **1b-NP** and **1ab-NP** were measured on a PTI Quantamaster spectrofluorometer. A JDS Uniphase 980 nm continues-wave laser diode (device type L4-9897510-100M) coupled to a 105 μm (core) fiber was employed as the excitation source. The output of the diode laser was collimated and directed through the sample perpendicular to the read-out plane of the fluorospectrometer using a Newport F-91-C1-T Multimode Fiber Coupler. All of the colloidal samples were held in a square quartz fluorescence cuvette (1 × 1 × 4.5 cm). All spectra were corrected for the instrument sensitivity. The fluorescence was recorded with a slit size of 1.5 nm, step size: 1 nm and integration: 0.1 nm. The power density of the 980 nm laser beam was adjusted from high to low by turning the focus dial on the laser mount. The laser beam defocus from a filled circle to a hollow ellipse by turning the dial 34 1/6 turns (focused beam: r = 0.3 mm, A = 0.028 cm^2 and 38 W cm^{-2}; defocused beam: a = 0.65 mm, b = 3 mm, A = 0.612 cm^2 and 2 W cm^{-2}).

Photochemistry

Ring-closing reactions for all dithienylethenes (**3a**, **3b**, **1a-NP**, **1b-NP** and **1ab-NP**) were carried out using the light source from a lamp used for visualizing TLC plates at 365 nm (Spectroline E-series, 15.9 mW cm^{-2}). Ring-opening reactions were carried out using a slide projector with a greater than 434 nm longpass filter (377 mW cm^{-2}) and a greater than 630 nm longpass filter (120 mW cm^{-2}). The samples were irradiated approximately 1–2 cm from the light source under scarce light conditions to eliminate interference from ambient light during the procedures. NIR to UV remote control ring-closing of **1a-NP**, **1b-NP** and **1ab-NP** were performed using a JDS Uniphase 980 nm laser diode (device type L4-9897510-100M) coupled to a 105 μm (core) fibre. The laser beam was collimated and directed horizontally through the sample using a Newport F-91-C1-T Multimode Fiber Coupler. The samples were magnetically stirred in fluorescence cuvettes (1 × 1 × 4.5 cm).

Emission quenching experiments

The percent emission quenching was calculated with Microsoft Excel software by calculating the area under each line segment of the emission graph by the formula: 0.5 × (wavelength 2 – wavelength 1) × (emission 2 + emission 1) followed by adding up all of the values for that specific wavelength or emission segment.

4-(4-(2-(5-(4-Methoxyphenyl)-2-methylthiophen-3-yl)cyclopent-1-en-1-yl)-5-methylthiophen-2-yl)phenol. A flame-dried round-bottom flask cooled under an N_2 atmosphere was charged with **2b** (100 mg, 0.21 mmol). Anhydrous CH_2Cl_2 (30 mL) was added *via* a cannula and the system was cooled in a dry-ice/acetone bath. The solution was treated with BBr_3 (0.34 mL, 3.60 mmol) drop-wise and was subsequently allowed to reach ambient temperature. The reaction was followed closely by TLC (1 : 1 EtOAc–hexanes, Rf: 0.7, pink upon 365 nm exposure) and after 30 min when most starting material was consumed, the solution was cooled to 0 °C and quenched with approximately 15 mL ice (exothermic). The reaction mixture was poured into a separatory funnel and diluted with saturated aqueous NH_4Cl and CH_2Cl_2. The phases were separated and the aqueous phase was extracted 3 times with CH_2Cl_2. The combined organic extracts were dried over anhydrous $MgSO_4$, vacuum-filtered and concentrated under reduced pressure. The product was purified by column chromatography (1 : 4 EtOAc–hexanes) and obtained as a colourless solid which turned pink upon exposure to UV light (75 mg, 76%). The compound rapidly decomposes at ambient temperature, store at −20 °C. Mp: 48–50 °C. ^{1}H NMR (500 MHz, CD_2Cl_2) δ 7.42 (d, J = 8.7 Hz, 2H), 7.37 (d, J = 8.6 Hz, 2H), 6.94 (s, 1H), 6.93 (s, 1H), 6.87 (d, J = 8.7 Hz, 2H), 6.80 (d, J = 8.6 Hz, 2H), 5.13 (s, 1H), 3.79 (s, 3H), 2.82 (t, J = 7.5 Hz, 4H), 2.05 (p, J = 7.5 Hz, 2H), 1.97 (s, 6H). ^{13}C NMR (126 MHz, CD_2Cl_2) δ 159.4, 155.5, 139.8, 139.7, 137.2, 135.1, 135.1, 133.9, 127.9, 127.8, 127.1, 126.9, 123.5, 116.0, 114.6, 55.8, 38.9, 23.5, 14.6. HRMS: Calculated for $C_{28}H_{26}O_2S_2$: $(M + H)^+$ 459.1374. Found: $(M + H)^+$ 459.1443.

5-(4-Methoxyphenyl)-2-methyl-3-(2-(2-methyl-5-(4-(prop-2-yn-1-yloxy)phenyl)thiophen-3-yl)cyclopent-1-en-1-yl)thiophene (3b). A round-bottom flask was charged with 4-(4-(2-(5-(4-methoxyphenyl)-2-methylthiophen-3-yl)cyclopent-1-en-1-yl)-5-methylthiophen-2-yl)phenol (63.9 mg, 0.14 mmol), K_2CO_3 (76.8 mg, 0.56 mmol), benzo-18-crown-6 (2.2 mg, 0.007 mmol), KI (1.2 mg, 0.007 mmol) and reagent grade acetone (10 mL). Propargylbromide (80 wt% in toluene, 31 mg, 0.21 mmol) was added and the system was equipped with a condenser and heated to reflux. After 18.5 h when the reaction was complete as indicated by TLC (1 : 3 EtOAc–hexanes, Rf: 0.52, pink upon 365 nm exposure), the reaction was cooled to ambient temperature, poured into a separatory funnel and diluted with EtOAc and saturated aqueous NH_4Cl. The phases were separated and the aqueous phase was extracted 3 times with EtOAc. The combined organic extracts were dried over anhydrous $MgSO_4$, vacuum-filtered and concentrated under reduced pressure. The product was purified by column chromatography (1 : 7 EtOAc–hexanes) and obtained as a colourless slightly sticky solid which turned pink upon exposure to UV light (59 mg, 86%). The compound was stored at −20 °C. Mp: 35–38 °C. ^{1}H NMR (500 MHz, CD_2Cl_2) δ 7.43 (t, J = 8.8 Hz, 4H), 6.95 (dd, J = 8.8, 2.4 Hz, 4H), 6.88 (s, 1H), 6.86 (s, 1H), 6.93 (d, J = 8.8 Hz, 2H), 6.86 (d, J = 8.8 Hz, 1H), 4.70 (d, J = 2.4 Hz, 2H), 3.80 (s, 3H), 2.84 (t, J = 7.5 Hz, 4H), 2.58 (t, J = 2.4 Hz, 1H), 2.08 (p, J = 7.5 Hz, 2H), 2.00 (s, 3H), 2.00 (s, 3H). ^{13}C NMR (126 MHz, CD_2Cl_2) δ 159.4, 157.2, 139.8, 139.5, 137.3, 137.2, 135.2, 135.1, 134.2, 133.9, 128.7, 127.7, 126.9, 123.8, 123.5, 115.6, 114.6, 79.0, 75.9, 56.3, 55. 8, 38.9, 23.5, 14.6, 14.6. HRMS: Calculated for $C_{31}H_{28}O_2S_2$: $(M + H)^+$ 497.1531. Found: $(M + H)^+$ 497.1614.

3-(3,3,4,4,5,5-Hexafluoro-2-(2-methyl-5-(4-(prop-2-yn-1-yloxy)-phenyl)-thiophen-3-yl)cyclopent-1-en-1-yl)-2-methyl-5-phenylthiophene (3a). Although the molecule has been reported earlier, this synthesis differs slightly and is therefore reported again here. A mixture of the phenol starting material[25] (644 mg, 1.2 mmol), K_2CO_3 (663 mg, 4.8 mmol), KI (10 mg, 0.06 mmol), benzo-18-crown-6 (19 mg, 0.06 mmol) and propargylbromide (208 mg, 1.4 mmol) and acetone (30 mL) was brought to reflux. After 20 h at reflux, the mixture was cooled to ambient temperature and quenched with saturated aqueous NH_4Cl, poured into a separatory funnel and diluted with EtOAc and treated with water. The phases were separated and the aqueous phase was extracted 3 times with EtOAc. The combined organic extracts were dried over $MgSO_4$, vacuum filtered and concentrated under reduced pressure. The product was purified by silica gel column chromatography (9.8 hexanes : 0.2 EtOAc) to yield a white solid (570 mg, 83%) which turned blue upon exposure to UV light. The compound was stored at −20 °C. ^{1}H NMR (500 MHz, $CDCl_3$) δ 7.54–7.51 (m, 2H), 7.48–7.45 (m, 2H), 7.39–7.35 (m, 2H), 7.30–7.28 (m, 1H), 7.26 (s, 1H), 7.16 (s, 1H), 7.00–6.96 (m, 2H), 4.70 (d, J = 2.4 Hz, 2H), 2.52 (d, J = 2.4 Hz, 1H), 1.94 (s, 3H), 1.93 (s, 3H).

Synthesis of a-NP. Approximately 150 mg of **o-NP** was dispersed in 8 mL of $CHCl_3$ and 2 mL of absolute EtOH and added to a 20 mL scintillation vial. In a separate vial, 3-azidopropylphosphonic acid[2] (500 mg) was dissolved in a mixture of $CHCl_3$ (2 mL) and absolute EtOH (2 mL). The 3-azidopropylphosphonic acid solution was then added to the nanoparticle dispersion *via* a Pasteur pipette. The resultant mixture was stirred overnight

at room temperature. The reaction solution was transferred to a centrifuge tube and hexanes were added until the mixture became cloudy. The reaction mixture was then centrifuged at 5000 rpm for 10 min and the supernatant was discarded. The precipitated nanoparticles were then redispersed in 5 mL of DMSO (3.8 wt%) for further experiments. FTIR (cm^{-1}): 2935, 2879, 2110 (strong, N_3), 1660, 1252, 1140, 1070, 920.

Synthesis of 2-component systems 1a-NP and 1b-NP. A solution of compound **3a** (3.47 mL of a stock solution of 6.0 mg, 0.01 mmol, 3.0×10^{-3} M in CH_3CN) or **3b** (3.83 mL of a stock solution of 5.2 mg, 0.01 mmol, 2.7×10^{-3} M in CH_3CN) was added to a 20 mL scintillation vial and the solvent was removed under reduced pressure. A dispersion of the azide nanoparticles **a-NP** (0.5 mL, 3.8 wt% in DMSO) was added to the vial and the mixture sonicated. The resulting clear dispersion was transferred to a 3 mL vial equipped with a stir-bar. Freshly prepared $CuSO_4 \cdot 5H_2O$ (24 μL, 1.04×10^{-4} mmol, 4.41×10^{-3} M in H_2O), sodium L-ascorbate (18 μL, 1.04×10^{-3} mmol, 5.75×10^{-2} M in H_2O), H_2O (8 μL) and Et_3N (10 μL) were added *via* calibrated auto-pipette and the reaction vessel was sealed and stirred at 35 °C for 24 h. The reaction mixture was transferred to a 1.5 mL Eppendorf tube and diluted with absolute EtOH (1 mL). After centrifugation (13 500 rpm, 30 min) the supernatant was discarded and the pellet redispersed in THF (1 mL) or CH_2Cl_2 (1 mL) for **3a** and **3b**, respectively, and centrifuged (13 500 rpm, 20 min). The supernatant was discarded and the pellet was redispersed in suitable solvent (2 mL), the clear colloidal dispersions (**1a-NP**: 3 wt% in THF, **1b-NP**: 2 wt% in CH_2Cl_2) were used for subsequent experiments without any further purification. Loading: **1a-NP**: 5000–7000 molecules per nanoparticle, **1b-NP**: 6000–8000 molecules per particle (Tables S1–S3‡). FTIR (cm^{-1}): **1a-NP**: 2964, 2928, 2855, 2360, 2110 (weak, N_3), 1655, 1515 (s), 1274, 1101, 1056, 988, 822. **1b-NP**: 2956, 2928, 2839, 2364, 2110 (weak, N_3), 1656, 1511, 1252, 1100, 1070, 1035, 824.

Synthesis of mixed 3-component system 1ab-NP. A mixture of compounds **3a** (1.73 mL of a stock solution of 3.0 mg, 0.005 mmol, 3.01×10^{-3} M in CH_3CN) and **3b** (1.92 mL of a stock solution of 2.6 mg, 0.005 mmol, 2.72×10^{-3} M in CH_3CN) was added to a 20 mL scintillation vial and the solvent was removed under reduced pressure. A dispersion of the azide nanoparticles **a-NP** (0.5 mL, 3.8 wt% in DMSO) was added, the mixture sonicated and the resulting clear dispersion was transferred to a 3 mL vial equipped with a stir-bar. Freshly prepared $CuSO_4 \cdot 5H_2O$ (11 μL, 1.0×10^{-4} mmol, 9.4×10^{-3} M in H_2O), sodium L-ascorbate (28 μL, 1.0×10^{-3} mmol, 3.79×10^{-2} M in H_2O), H_2O (11 μL) and Et_3N (10 μl) were added *via* auto-pipette and the reaction vessel was sealed and stirred at 35 °C for 24 h. The reaction mixture was transferred to a 1.5 mL Eppendorf tube and diluted with absolute EtOH (1 mL). After centrifugation (13 500 rpm, 30 min) the supernatant was discarded and the pellet redispersed in THF (1 mL) and centrifuged (13 500 rpm, 20 min). The supernatant was discarded and the pellet was redispersed in THF (2 mL). The slightly hazy colloidal dispersion (2 wt%) was used for subsequent experiments without any further purification. FTIR (cm^{-1}): **1ab-NP** 2959, 2997, 2940, 2362, 2110 (weak, N_3), 1654, 1515, 1251, 1114, 1056, 989, 824.

Acknowledgements

This research was supported by the Natural Sciences and Engineering Research Council (NSERC) of Canada, the Canada Research Chairs Program, and Simon Fraser University through funding from the Community Trust Endowment Fund. This work made use of 4D LABS shared facilities supported by the Canada Foundation for Innovation (CFI), British Columbia Knowledge Development Fund (BCKDF) and Simon Fraser University. J.-C. Boyer thanks the Michael Smith Foundation for Health Research for support. C.-J. Carling thanks Simon Fraser University for a Graduate Fellowship.

Notes and references

1 I. Yildiz, E. Deniz and F. M. Raymo, *Chem. Soc. Rev.*, 2009, **38**, 1859–1867.
2 J. Cusido, E. Deniz and F. M. Raymo, *Eur. J. Org. Chem.*, 2009, 2031–2045.
3 M.-Q. Zhu, L. Zhu, J. J. Han, W. Wu, J. K. Hurst and A. D. Q. Li, *J. Am. Chem. Soc.*, 2006, **128**, 4303–4309.
4 L. Zhu, W. Wu, M.-Q. Zhu, J. J. Han, J. K. Hurst and A. D. Q. Li, *J. Am. Chem. Soc.*, 2007, **129**, 3524–3526.
5 J. Fölling, S. Polyakova, V. Belov, A. van Blaaderen, M. L. Bossi and S. W. Hell, *Small*, 2008, **4**, 134–142.
6 Z. Hu, Q. Zhang, M. Xue, Q. Sheng and Y.-G. Liu, *Opt. Mater.*, 2008, **30**, 851–856.
7 M. Tomasulo, E. Deniz, R. J. Alvarado and F. M. Raymo, *J. Phys. Chem. C*, 2008, **112**, 8038–8045.
8 Z. Zhou, H. Hu, H. Yang, T. Yi, K. Huang, M. Yu, F. Li and C. Huan, *Chem. Commun.*, 2008, 4786–4788.
9 Z. Erno, I. Yildiz, B. Gorodetsky, F. M. Raymo and N. R. Branda, *Photochem. Photobiol. Sci.*, 2010, **9**, 249–253.
10 C. Zhang, H.-P. Zhou, L.-Y. Liao, W. Feng, W. Sun, Z.-X. Li, C.-H. Xu, C.-J. Fang, L.-D. Sun, Y.-W. Zhang and C.-H. Yan, *Adv. Mater.*, 2010, **22**, 633–637.
11 J. Chen, P. Zhang, G. Fang, P. Yi, X. Yu, X. Li, F. Zeng and S. Wu, *J. Phys. Chem. B*, 2011, **115**, 3354–3362.
12 I. Yildiz, S. Impellizzeri, E. Deniz, B. McCaughan, J. F. Callan and F. M. Raymo, *J. Am. Chem. Soc.*, 2011, **133**, 871–879.
13 L. Cheng, K. Yang, M. Shao, S.-T. Lee and Z. Liu, *J. Phys. Chem. C*, 2011, **115**, 2686–2692.
14 J.-C. Boyer, C.-J. Carling, S. Y. Chua, D. Wilson, B. Johnsen, D. Baillie and N. R. Branda, *Chem.–Eur. J.*, 2012, **18**, 3122–3126.
15 *Organic Photochromic and Thermochromic Compounds*, ed. J. C. Crano and R. J. Guglielmetti, Plenum, New York, 1999.
16 S. H. Nam, Y. M. Bae, Y. I. Park, J. H. Kim, H. M. Kim, J. S. Choi, K. T. Lee, T. Hyeon and Y. D. Suh, *Angew. Chem., Int. Ed.*, 2011, **50**, 6093–6097.
17 Coating nanoparticles with a biocompatible material reduces the toxicity but does not eliminate 'blinking'. (*a*) M. Bruchez Jr., M. Moronne, P. Gin, S. Weiss and A. P. Alivisatos, *Science*, 1998, **281**, 2013–2016; (*b*) W. C. W. Chan and S. Nie, *Science*, 1998, **281**, 2016–2018; (*c*) X. Michalet, F. F. Pinaud, L. A. Bentolila, J. M. Tsay, J. J. Li, G. Sundaresan, A. M. Wu, S. S. Gambhir and S. Weiss, *Science*, 2005, **307**, 538–544.
18 S. Wu, G. Han, D. J. Milliron, S. Aloni, V. Altoe, D. V. Talapin, B. E. Cohen and P. J. Schuck, *Proc. Natl. Acad. Sci. U. S. A.*, 2009, **106**, 10917–10921.
19 L. Cheng, K. Yang, M. Shao, X. Lu and Z. Liu, *Nanomedicine*, 2011, **6**, 1327–1340.
20 D. K. Chatterjee and Y. Zhang, *Nanomedicine*, 2008, **3**, 73–82.
21 H. S. Mader, P. Kele, S. M. Saleh and O. S. Wolfbeis, *Curr. Opin. Chem. Biol.*, 2010, **14**, 582–596.
22 M. Irie, in *Molecular Switches*, ed. B. L. Feringa, Wiley-VCH, Weinheim, Germany, 2001.

23 J.-C. Boyer, C.-J. Carling, B. D. Gates and N. R. Branda, *J. Am. Chem. Soc.*, 2010, **132**, 15766–15772.
24 J. Finden, T. Kunz, N. R. Branda and M. O. Wolf, *Adv. Mater.*, 2008, **20**, 1998–2002.
25 A. J. Myles, T. J. Wigglesworth and N. R. Branda, *Adv. Mater.*, 2003, **15**, 745–748.
26 J. J. D. de Jong, L. N. Lucas, R. Hania, A. Pugzlys, R. M. Kellogg, B. L. Feringa, K. Duppen and J. H. van Esch, *Eur. J. Org. Chem.*, 2003, 1887–1893.
27 A. K. Tucker-Schwartz and R. L. Garrell, *Chem.–Eur. J.*, 2010, **16**, 12718–12726.
28 See ESI‡ for details.
29 H. S. Mader, M. Link, D. E. Achatz, K. Uhlmann, X. Li and O. S. Wolfbeis, *Chem.–Eur. J.*, 2010, **16**, 5416–5424.
30 Although most of the photochromic studies on the free ligands were carried out using CH_3CN solutions, we did not observe any changes in the spectra when they were measured in THF (for **1a-NP**) and CH_2Cl_2 (for **1b-NP**). See Fig. S3 in the ESI‡ for details.
31 Photoswitch **3b^c** and **1b^c-NP** degrades during UV light irradiation and the original spectra is not fully regenerated upon >434 nm irradiation, see Fig. S9‡ for details.
32 The concentrations of the photoswitches were estimated by comparing the absorbances for solutions of the hybrid systems (**1a-NP** and **1b-NP**) to the free ligands in the same solvent. This assumes that the photostationary states are the same. See the ESI‡ for details.
33 When a >434 nm filter is placed between the cuvette and the detector, the 670–750 nm emissions are not present in the spectra indicating that these emission are due to the second order diffraction off the emission monochromator grating of the UV emissions from Tm^{3+}.
34 W. Wu, L. Yao, T. Yang, R. Yin, F. Li and Y. Yu, *J. Am. Chem. Soc.*, 2011, **133**, 15810–15813.
35 Y. Yang, Q. Shao, R. Deng, C. Wang, X. Teng, K. Cheng, Z. Cheng, L. Huang, Z. Liu, X. Liu and B. Xing, *Angew. Chem., Int. Ed.*, 2012, **51**, 3125–3129.
36 All the spectra for these studies can be found in the ESI.‡.
37 For additional information, see Fig. S11 in the ESI.‡.
38 C.-J. Carling, J.-C. Boyer and N. R. Branda, *J. Am. Chem. Soc.*, 2009, **131**, 10838–10839.
39 C.-J. Carling, F. Nourmohammadian, J.-C. Boyer and N. R. Branda, *Angew. Chem., Int. Ed.*, 2010, **49**, 3782–3785.
40 B. Yan, J.-C. Boyer, N. R. Branda and Y. Zhao, *J. Am. Chem. Soc.*, 2011, **133**, 19714–19717.
41 C.-J. Carling, J.-C. Boyer and N. R. Branda, unpublished results.